On the significance of the climate-dataset time resolution in characterising wind-driven rain and simultaneous wind pressure. Part I: Scalar approach

José M. Pérez-Bella[1], Javier Domínguez-Hernández[1,*], Enrique Cano-Suñén[1], Juan J. del Coz-Díaz[2], Mar Alonso-Martínez[2]

[1] *Department of Construction Engineering, Engineering and Architecture School, University of Zaragoza, María de Luna s/n, 50018, Zaragoza, Spain.*

E-mails: jmpb@unizar.es, javdom@unizar.es and ecs@unizar.es

[2] *Department of Construction Engineering, University of Oviedo, Edificio Departamental Viesques nº 7, 33204 Gijón, Spain.*

E-mails: juanjo@constru.uniovi.es and mar@onstru.uniovi.es

* **Corresponding author:** Dr. Javier Domínguez-Hernández.

Department of Construction Engineering, University of Zaragoza,

Campus Río Ebro, Edificio Betancourt, María de Luna s/n, 50018, Zaragoza, Spain.

Tel.Fax: +34 976 76 21 00. E-mail: javdom@unizar.es

Acknowledgements

This work was partially financed by the Spanish Ministry of Science and Innovation and the FICYT co-financed with FEDER funds under the Research Projects BIA2012-31609 and FC-15-GRUPIN14-004.

On the significance of the climate-dataset time resolution in characterising wind-driven rain and simultaneous wind pressure. Part I: Scalar approach

Abstract

The joint action of wind-driven rain and wind pressure is the main cause of water penetration in building facades, which causes various habitability and durability problems. The most widespread characterisation of both climate factors is based on exposure indices calculated in free-field conditions from records of precipitation - wind speed (scalar indices), adding wind direction for directional indices. The time resolution of this climate dataset defines the calculation effort and the accuracy obtained, and average daily, monthly, or annual records are typical due to their greater availability. This paper investigates the influence of this time resolution on the accuracy of these scalar exposure indices (driving rain index, hereafter aDRI, and driving-rain wind pressure, hereafter DRWP) by assessing the nature and magnitude of errors associated with different averaged records. For this purpose, 10-min, hourly, daily, monthly and annual meteorological data collected over 15 years in 6 Spanish weather stations at locations characterised by different environments and topography are analysed. In addition, relationships capable of adjusting indices of any time resolution to an accuracy similar to that reached through 10-min records are proposed. In general, the value of driving-rain wind pressure exhibits greater sensitivity than the driving rain index at this time resolution, incorporating significant errors even with daily datasets. In turn, the use of monthly and annual records should be reconsidered, given their high uncertainty. The results demonstrate how the daily datasets for aDRI indices and hourly datasets for DRWP values are sufficient to characterise these exposures with errors of less than 11%.

Keywords

Weather measurements; Climatic exposure; Error analysis; Building façades; Water penetration

1. Introduction

Rainwater penetration into facade materials causes various durability problems, such as erosion, corrosion, frost attack, salt crystallisation, surface soiling and discoloration, loss of adherence, deformations, cracking, and falling materials (D'Ayala and Aktas 2016; De Souza, Bauer, Nascimento, Capuzzo and Zanoni 2016; Erkal, D'Ayala and Sequeira 2012; Hall and Hoff 2012; Tang, Davidson, Finger and Vance 2004). It is also one of the main factors affecting the hygrothermal performance of the building, reducing its thermal insulation and increasing energy consumption and emission of air pollutants (Dell'Isolla, D'Ambrosio, Giovinco and Ianeiello 2013; Gutiérrez, Gutiérrez and Nafidi 2008; Kočí et al. 2017; Nascimento, Bauer, de Souza and Zanoni 2016). In addition, this moisture is associated with different health problems for the tenants (World Heatlh Organization 2011).

The penetration of atmospheric water is produced by a combination of rainwater impinging on the facade and the action exerted by the wind on this water supply. The rain diverted by wind action (wind-driven rain, hereafter WDR) and the simultaneous driving-rain wind pressure (DRWP) are thus the main climatic factors involved in the penetration process (Blocken, Derome and Carmeliet 2013; Cornick and Lacasse 2005; Sahal and Lacasse 2004). Determining both parameters is a necessary task to evaluate the characteristic exposure conditions in each site and to identify the extreme situations that should define facade designs that guarantee the necessary watertightness. For the latter, it is preferable to analyse the exposure values associated with extreme conditions of wind and rainfall, based on return periods (Mornet, Opitz, Luzi, Loisel and Bailleul 2016;Van de Vyver 2015).

The most widespread and functional method for determining WDR exposure is based on semi-empirical approaches, establishing experimental adjustments from wind and precipitation measurements collected under free-field conditions (Lacy and Shellard 1962; Straube and Burnett 2000). Thus, it is possible to define "airfield" indices associated with each location (i.e., relative to free-field conditions), which can subsequently be refined using empirical coefficients to represent the specific conditions of each façade,

such as surroundings, topography, and geometry (American Society of Heating and Air-Conditioning Engineers 2009; European Committee for Standardization 2009).

The study of DRWP has received much less attention than WDR exposure, despite its crucial role in the penetration process, reflected in the standardised watertightness tests (American Architectural Manufacturers Association 2005; American Society for Testing and Materials 2009; European Committee for Standardization 2001; Lacasse, O'Connor, Nunes and Beaulieu 2003). The few studies performed have used the Bernoulli equation to determine the DRWP value, considering only the wind speed records concurrent with precipitation events (Pérez, Domínguez, Cano, del Coz, Martín 2014; Pérez, Domínguez, Rodríguez, del Coz and Cano 2013; Welsh, Skinner and Morris 1989).

The WDR and DRWP exposure indices can be scalar (representing the overall exposure value at the site) or directional by also evaluating wind direction data to determine the exposure on each possible facade orientation (Blocken and Carmeliet 2004). The directional results provide more comprehensive information but also require a greater calculation effort and access to additional weather data, which are not always available.

In this sense, the time resolution of the climatic data constitutes another important limitation that decisively influences the accuracy of the exposure indices. The climate datasets conventionally used to characterise these exposures (daily, monthly and annual) are obtained as arithmetic averages of raw measurement data generally not available (collected every 1, 5, and 10 min). In turn, these raw data reflect the linearisation of the meteorological sensor outputs (World Meteorological Organization 2008). Thus, these arithmetic means are a source of co-occurrence and averaging errors, due to omitting the actual simultaneity of wind with rainfall periods and to the mathematical averaging of the raw data, respectively (Blocken and Carmeliet 2007, 2008; Pérez, Domínguez, Rodríguez, del Coz and Cano 2012; Skerlj 1999).

Some studies have addressed the required time resolution of these datasets for WDR calculations based on computational fluid dynamics (CFD), focusing their efforts on proposing improved averaging techniques for the raw measurement data (Blocken and Carmeliet 2007, 2008). However, Ge (2015) has demonstrated that these improved techniques are not suitable to semi-empirical calculation methods. Thus, a systematic approach that determines the errors associated with the use of datasets with different time resolution has not yet been developed for semi-empirical calculations of WDR exposure (much less for DRWP exposure). Consequently, there are currently no guidelines to evaluate the accuracy and uncertainty of multiple studies conducted using datasets with low time resolution.

This article develops an exhaustive analysis of 10-min records collected between 2001 and 2016 in 6 meteorological stations in the northwest of Spain, obtaining airfield exposure indices of WDR and DRWP based on 10-min, hourly, daily, monthly and annual datasets. This analysis aims to reduce this lack of information, offering a broad perspective on the nature and magnitude of errors associated with each datasets'time resolution for locations with different characteristics. In addition, general adjustment relations between the indices calculated from each dataset of different time resolution are proposed. For clarity and given the diverse climatic data involved, this study is divided into two distinct parts: the investigation of the significance of the datasets time resolution on the scalar results (Part I) and on the directional results (Part II).

2. Background

Characterisation of the WDR exposure at sites can be performed by means of experimental measurements, CFD methods and semi-empirical correlations (Blocken and Carmeliet 2004; Hangan 1999). Experimental measurements are costly and entail long periods of observation. In turn, CFD methods require a significant calculation effort and high-quality input data adapted to each specific

situation. Only semi-empirical methods allow a simple and functional characterisation of the exposure in a large number of sites, although their thoroughness is inferior to the other methods.

These semi-empirical methods are based on the 'WDR relationship', which uses free-field climate records generally gathered at most of the weather stations and empirically fitted coefficients (Hoppestad 1955; Lacy and Shellard 1962). By multiplying simultaneous records of wind speed U (m/s) and precipitation intensity R_h (l/m^2), this relationship allows estimation of an airfield WDR value (l/m^2), using the value α (s/m) as a coefficient physically related to the terminal falling velocity of raindrops and that depends on the intensity of precipitation at each time point (Eq. 1) (Cornick, Dalgliesh, Said, Djebbar, Tariku and Kumaran 2002; Straube and Burnett 2000).

$$WDR = F_{wall\ indices} \cdot \alpha \cdot U \cdot R_h \quad [1]$$

Standards such as ISO 15927-3 or ASHRAE 160 also incorporate dimensionless coefficients (grouped here under the designation $F_{wall\ indices}$) to represent the complex interaction among wind, rain and the building, thus determining the WDR exposure on each specific facade based on its shape (e.g., height, cover, and geometry), the terrain roughness, the topography of the surroundings and nearby obstructions (American Society of Heating and Air-Conditioning Engineers 2009; European Committee for Standadization 2009). To ensure the representativeness of the results, the calculation should be performed by averaging at least 10 years of climate data (as stated in ISO standard 15927-3).

By also incorporating simultaneous records of wind direction D (º), it is possible to determine the directional distribution of the exposure in each facade orientation θ (º). For this, Eq. 1 would be multiplied by cos(D-θ), thus considering only the wind direction records when the analysed facade is in a leeward position (cosine projection with positive value). In this work, scalar indices refer to those exposure values that do not incorporate climate records of wind direction, thus providing only global (non-directional) exposure information.

Based on this WDR relationship, the annual driving-rain index (aDRI) is the simplest and most generalised indicator to evaluate the average annual exposure at each location (Akingbade 2004; Chand and Bhargava 2002; Domínguez, Pérez, Alonso, Cano and del Coz 2016; Giarma and Aravantinos 2011). For its scalar calculation, the coefficient α, directional characterisation and wall indices (i.e., obtaining an airfield index) are ignored. This gives an *aDRI* value (m^2/s), which qualitatively characterises the scalar exposure from the *k* records collected at the site over *N* years (see Eq. 2). The divider 1000 allows the conversion of l/m^2 (i.e., mm of precipitation) in m, thus simplifying the units of the index. In spite of its simplicity, this index can be used as reference to obtain more refined results, incorporating adequate values for the coefficient α and the wall indices.

$$aDRI = \frac{\sum_{i=1}^{k} U_i \cdot \left(\frac{R_{h\,i}}{1000} \right)}{N} \qquad [2]$$

On the other hand, the penetration of water into building facades does not depend exclusively on the water supply provided by wind-driven rain. On the contrary, it depends strongly on the simultaneous existence of wind pressure on the facade that is capable of overcoming the surface tension and capillary pressure of the water contained in the material deficiencies. Thus, it is estimated that this is the most sensitive parameter related to water penetration in facades without openings and pores greater than 1 mm (Cornick and Lacasse 2005). Therefore, characterising the wind pressure that usually acts simultaneously to the rainfall at the location (i.e., DRWP) is of equal interest to studying the WDR.

The most widespread method of determining the value of *DRWP* (Pa) is based on the analysis of the *m* wind speed records *U* (m/s), which are simultaneous to precipitation during the studied period ($m \leq k$). This is performed using the Bernoulli equation (Eq. 3), where C_p (-) represents the pressure coefficient (usually equal to 1) and ρ_{air} the air density (generally set at 1.2 kg/m^3). As in Eq. 2, this result represents the scalar exposure associated with the site (in free-field conditions), and the factor cos(D-θ) can also be incorporated to obtain the directional distribution of the DRWP exposure.

$$DRWP = \frac{\sum_{i=1}^{m} C_p \cdot \frac{1}{2} \cdot \rho_{air} \cdot U_i^{\,2}}{m} \quad [3]$$

In both equations (Eqs. 2 and 3), it is possible to use climate data with different time resolutions, without there being uniformity in the studies developed so far (Akingbade 2004; Blocken and Carmeliet 2004; Chand and Bhargava 2002; Cornick and Lacasse 2005; Domínguez et al. 2016; Giarma and Aravantinos 2011; Pérez et al. 2014; Pérez, Domínguez, Cano, del Coz and Alonso 2013; Pérez, Domínguez, Rodríguez et al. 2012, 2013). On the contrary, in each case, the available climate records (usually annual, monthly or daily data) have been used. However, the selected time resolution influences the accuracy of the results by incorporating two types of errors in the exposure indices: a co-occurrence error (e_1), which is due to not exhaustively recording the simultaneity of wind and precipitation events, and an averaging error (e_2), which is due to the smoothing of the values of the climatic variables when averaging of the raw data (Blocken and Carmeliet 2007, 2008).

To these errors other uncertainties must be added, which are associated with the collection of records through the meteorological sensor outputs: small-scale variability of the atmosphere conditions, noise in electronic devices, precipitation gauge errors, disturbances in wind measurements due to topographic effects and random instrumental errors among others. These random uncertainties can be minimised by collecting the sensor outputs as 2- to 10-min averages, recording wind data at 10 m above ground level in an open field (free-field conditions), and using recording precipitation gauges with high resolution (World Meteorological Organization 2008). In this sense, the 10-min records ensure a good representation of the rapid variations that characterise precipitation and wind phenomena (Jones and Sims 1978; Sumner 1988; Van der Hoven 1957).

Blocken and Carmeliet (2007, 2008) have proposed weighted averaging techniques for the raw measurement data, obtaining climate datasets to calculate with less error the WDR exposure using CFD methods. However, a recent study has shown that these weighted techniques reduce the accuracy of semi-

empirical calculations (Ge 2015). Assessing climate records collected over 6-12 months in 3 Canadian cities, this study also identified an average error close to 12% in the WDR airfield indices obtained from hourly datasets, compared to those calculated using 5- and 10-min records. However, the errors associated with other conventional datasets'time resolutions (daily, monthly, and annual) were not analysed, nor was the nature of the error (e_1 and e_2) differentiated. Using 30 years of daily records in 80 Spanish locations, another study quantified the e_1 and e_2 errors present in the monthly and annual airfield indices of WDR (with respect to their daily equivalents), concluding that both sources of error were equal and similar in the monthly and annual indices (Pérez, Domínguez, Rodríguez et al. 2012). The same study was performed in 41 Greek cities, obtaining analogous results, although with a higher prevalence of averaging error (Giarma and Aravantinos 2014).

All of these studies are partial approximations to the problem in which the climatic series are not very representative, or the analysis of the most conventional time resolutions is obviated (mainly monthly and annual), or the error with respect to recording intervals sufficiently exhaustive (e.g., 10-min records) is not identified. In addition, none of them analyses the effect of the time resolution of the dataset on the DRWP characterisation. Consequently, to the best of the authors' knowledge, a systematic study that comprehensively characterises the effect of the time resolution of the dataset on the accuracy of the semi-empirical airfield indices of both WDR and DRWP exposures has not yet been conducted.

Thus, guidelines to assess the real accuracy of the exposure results obtained from datasets of low time resolution are lacking. Given that these studies are the most common (due to the difficulty in accessing hourly data with the representativeness required by ISO 15927-3 and ASHRAE 160~~P~~ standards), most of the published characterisations for both exposures have been performed without knowing their real uncertainty range. Similarly, although adjustment relationships have been defined between daily, monthly and annual exposure indices, extrapolations to achieve an accuracy similar to that of the indices based on raw measurement data have not yet been developed.

To clarify these issues, this paper analyses hourly, daily, monthly and annual climate records, identifying the nature and magnitude of the errors associated with the use of climatic datasets of each time resolution in the scalar airfield indices defined by Eqs. 2 and 3. To compare and assess these errors, the exposure values calculated from 10-min records are taken as a reference. In addition, adjustment relationships to extrapolate results with an accuracy similar to that defined by 10-min records from the indices obtained through any time resolution of the dataset are proposed. The validity of these results should be circumscribed to areas with climatic conditions and exposure levels similar to those analysed, and future studies will be still necessary to refine them under distinct operating conditions.

3. Error assessment in the scalar characterisation of WDR and DRWP airfield indices

3.1 Research scope

The increasing deployment of automatic weather stations equipped with data-loggers capable of collecting and transmitting raw data in real time (or storing them until download) offers new possibilities to incorporate better-time-resolution records in the calculations previously described.

For this study, 6 automatic stations installed since 2000 in the northwest of Spain (Galicia region) have been selected (see Fig. 1). The choice of these stations is justified by the availability of sufficiently representative meteorological datasets, which has allowed the examination of 15 years of records in all of them (1 Feb. 2001 – 31 Jan. 2016). At each station, more than 780,000 10-min intervals have been analysed, with simultaneous records of precipitation intensity and wind speed (measured at 10 m above open flat ground). Less than 1.5% of the analysed intervals lack records, as a result of failures, problems with data transmission or storage, maintenance, etc., which guarantees the representativeness of the historical series. The reliability and longevity of these datasets ensure that the results obtained are not influenced by years of exceptional climatology nor by prolonged interruptions of the records.

The devices used to record these climatic variables conform to the guidelines set by the World Meteorological Organisation (2008) and form part of the official meteorological network of the region of Galicia (Xunta of Galicia 2017). To obtain the dataset corresponding to other usual time resolutions (e.g., hourly, daily, monthly and annual), 10-min records have been arithmetically added and averaged using a spreadsheet program.

Fig. 1. Characteristics and location of the 6 analysed weather stations.

Bordered by the Atlantic Ocean on its northern and western boundaries (see Fig. 2), Galicia presents the highest WDR and DRWP exposures in Spain, especially near the coast and the numerous ocean-drowned river valleys (Pérez et al. 2014; Pérez, Domínguez, Rodríguez et al. 2012, 2013). The west coast and the interior of the region are characterised by a topography of low hills and subject to strong winds from the Atlantic Ocean. It also has an oceanic climate with dispersed precipitation throughout the year and seasonally more intense (in autumn and winter). In northern and eastern Galicia, the more rugged topography (reaching elevations of up to 2,100 m near the O Invernadeiro station) reduces the influence of the ocean on the local climate. This makes possible the existence of a warm-summer Mediterranean climate, with more concentrated rainfall in autumn and winter (Kottek, Grieser, Beck, Rudolf and Ruber 2006).

Fig. 2. Location of the 6 weather stations selected for the conducted study. *Darker colours represent higher elevations.*

In addition to this climatic variety and high exposure, the 6 stations are characterised by different environmental conditions, elevation, topography and distance to the coast. Two of the stations correspond to coastal locations (CIS Ferrol and Corrubedo) located less than 1 km from the ocean and at low elevation. CIS Ferrol is also located in the important Ría de Ferrol (a wide ocean-drowned river valley), bordered by low hills. The Pedro Murias station is located in the area of other small estuary denoted Ría de Ribadeo less than 4 km from the coast and on a flat terrain. Above 350 m of elevation, the stations of Queimadelos and Campus Lugo are located in wooded and urban environments, respectively. The last station is located at 1,026 m elevation, in the mountains of the interior belonging to the Natural Park O Invernadeiro.

The stations located close to the coast and subjected to strong ocean winds are highly exposed to wind (mean wind speed of 4.09 m/s in Pedro Murias and 3.17 m/s in CIS Ferrol, for the period considered), whereas for stations located inland, only O Invernadeiro reaches 2.30 m/s (due to its higher elevation). The Queimadelos station, at 371 m and in a wooded environment, presents the lowest wind exposure (mean wind speed of 1.37 m/s). There are also significant rainfall variations, ranging from 948 mm/year in Campus Lugo to 1,785 mm/year in Queimadelos (considering the 15 years studied). The O Invernadeiro station, due to its altitude, also has a high rainfall (1,651 mm/year). Altogether, this variety of conditions provides representative results for different types of locations and exposure levels analogous to those of these stations.

3.2 Calculations and results

Using the climate datasets associated with different time resolutions, the scalar exposure indices described in Eqs. 2 and 3 have been calculated for each location. For clarity, each exposure index is prefixed with an acronym *j* to represent the time resolution of the dataset used in its calculation (i.e., "*h*" for hourly

calculations, "*d*" for daily, "*m*" for monthly and "*a*" for annual). Thus, the values used as reference (based on 10-min records) are denoted as *10'aDRI* and *10'DRWP*. These results are presented in Table 1.

Table 1.
Exposure results to wind-driven rain and simultaneous wind pressure for climate datasets of different time resolution.

These exposure indices are consistent with those identified in 2014 by another study conducted in the region of Galicia, which produced two exposure isopleth maps from daily records collected at 80 stations (Pérez et al. 2014). Only Campus Lugo, with a value of 2.06 m^2/s, slightly exceeds the range 0-2 m^2/s indicated by the daDRI isopleth map for its area. Likewise, only the dDRWP value from O Invernadeiro (5.10 Pa), exceeds the range of 0-5 Pa marked by the isopleth exposure map for its zone. This consistency with previous results reinforces the validity of the values presented in Table 1.

However, the presented values show that the exposure calculated using datasets with a higher time resolution (and that are therefore more accurate and realistic) is higher to that identified by the daDRI and dDRWP indices. It follows that the exposure characterisation provided by these exposure maps, like many others available in the bibliography and obtained from low-time-resolution records, need additional corrections to avoid underestimating the actual exposure in the sites. Quantifying the magnitude of these underestimates according to the time resolution used in the calculation is therefore a key factor to improve the accuracy of this type of study.

To analyse the nature of the errors associated with each time resolution *j*, the same previous calculation has been repeated (Eqs. 2 and 3), but those 10-min wind records corresponding to intervals without precipitation were removed from the hourly, daily, monthly and annual averages. The result eliminates the co-occurrence error, obtaining exposure indices in which only the averaging error e_2 (see Table 2)

appears. For clarity, the subscript e_2 is incorporated into these refined exposure values (without co-occurrence error).

Table 2.
Exposure results without co-occurrence error for climate datasets with different time resolutions.

The difference between the 10-min exposure values and the values thus refined for each time resolution *j* allows the estimation of the characteristic averaging error at each dataset time resolution (e_2). The e_1 error can then be obtained as the difference between the total error (i.e., $e_1 + e_2$) and the error linked exclusively to the mathematical averaging of the climate records, e_2 (Eqs. 4-8). The results of this analysis are presented in Table 3 (expressed as percentages).

$$_{j}aDRI\ error\ \left(e_1+e_2\right)=\frac{100\cdot\left(_{j}aDRI-10'aDRI\right)}{10'aDRI} \quad [4]$$

$$_{j}aDRI\ error\ e_2=\frac{100\cdot\left(_{j}aDRI_{e2}-10'aDRI\right)}{10'aDRI} \quad [5]$$

$$_{j}DRWP\ error\ \left(e_1+e_2\right)=\frac{100\cdot\left(_{j}DRWP-10'DRWP\right)}{10'DRWP} \quad [6]$$

$$_{j}DRWP\ error\ e_2=\frac{100\cdot\left(_{j}DRWP_{e2}-10'DRWP\right)}{10'DRWP} \quad [7]$$

$$error\ e_1=error\left(e_1+e_2\right)-error\ e_2 \quad [8]$$

Table 3.
Percentage errors derived from the non-co-occurrence of wind and rain (e_1) and from the averaged data (e_2) for climate datasets of different time resolution (regarding 10-min values).

As expected, the magnitude of the errors increases with decreasing time resolution of the climate dataset. However, this growth is not proportional to the time resolution, nor are the errors similar in both exposure indices for the same time resolution of the dataset. Nor do the factors causing the error have the same influence on the different time resolutions (see Figs. 3 and 4). It is also observed that although both e_1 and e_2 tend to underestimate the existing exposure, in the case of hourly datasets, both sources of error can counteract each other, thus reducing the resulting error.

Fig. 3. Magnitude and nature of the aDRI error associated with each time resolution and its fluctuation for the different analysed locations.

Fig. 4. Magnitude and nature of the DRWP error associated with each time resolution and its fluctuation for the different analysed locations.

4. Discussion

By analysing the results presented in Table 1, it can be observed that the sites subjected to a greater mean wind speed also exhibit higher values of 10'DRWP exposure (see Fig. 1). This correlation is consistent with the high coefficients of determination R^2 identified between values of DRWP and wind pressure in different countries (Domínguez et al. 2016; Pérez, Domínguez, Cano et al. 2013; Pérez et al. 2014). However, site rainfall amount is not the only relevant factor in estimating the aDRI value, making a specific analysis of precipitation and simultaneous wind records to determine the WDR exposure unavoidable (e.g., Corrubedo exhibits the highest aDRI value but an intermediate pluviometry; Queimadelos exhibits an intermediate aDRI value but the highest precipitation).

The maximum values of WDR and DRWP exposure are identified at stations closest to the coast (Corrubedo 7.98 m^2/s and 40.82 Pa, respectively), thus presenting a greater risk of water penetration in

the facades. Pedro Murias and Queimadelos, somewhat further from the coast, have lower WDR exposures than Corrubedo and CIS Ferrol. Campus Lugo, in an urban environment in the interior of Galicia, exhibits the lowest aDRI value (2.23 m^2/s). Despite its distance to the coast, O Invernadeiro reaches a 10'aDRI value of 5.39 m^2/s, due to its elevation and high rainfall. In contrast, its DRWP value is lower than that of the coastal stations. In this sense, the lowest values of DRWP exposure occur in stations characterised by their urban and forest environment: Campus Lugo (4.20 Pa) and Queimadelos (3.57 Pa).

Considering the errors associated with the use of climatic datasets of each time resolution (Figs. 3-6), it is observed that the use of hourly datasets introduces an average error of 1.46% and 10.48% in the WDR and DRWP exposure values, respectively. In any case, the error varies between the analysed stations, depending on the particular characteristics of the atmospheric events at each site. Thus, the standard deviations σ for haDRI and hDRWP values reach 1.2% and 4.9%, respectively. In the case of daily datasets, the mean errors increase to 8.15% for the WDR values (still below the error associated with the hDRWP value) and 37.62% for the dDRWP values. Similar to the hourly errors, the variability is also significant (σ is equal to 4.0% for the daDRI indices and 10.7% for the dDRWP indices).

For their part, the monthly and annual datasets introduce very high errors in the scalar characterisation of the exposure, without there being a significant difference in accuracy between these two time resolutions. Thus, the mean error for the maDRI values reaches 28.87% (σ = 8.8%) and is 31.83% for the aaDRI indices (σ = 10.6%). In the case of DRWP exposure, the mean error of the mDRWP values reaches 57.92% (σ = 10.1%), and that of aDRWP values reaches 59.47% (σ = 9.9%).

As observed, in general, the error associated with aDRI values is significantly less than that identified in the DRWP indices for the same time resolution of the dataset. This fact can be explained by the different number of climatic variables involved in each exposure index, and by their variability during precipitation periods. In calculating the DRWP value, the magnitude of the error depends on the influence of the co-occurrence and averaging errors on a single variable (wind speed). This meteorological dataset is highly

variable, so it is especially sensitive to the averaging error. However, the aDRI index results from the product between this wind speed dataset and the simultaneous precipitation data at each lapse. This weighting reduces the sensitivity to the averaging error and also minimises the co-occurrence error: even if a wind speed datum not simultaneous to precipitation is considered, its associated precipitation datum (zero) does not contribute to the total precipitation, thus reducing the influence of this wind datum in the daDRI value calculation. For example, by assuming a hypothetical interval of temporal resolution composed by 6 raw data (5 of which do not present precipitation), the total precipitation will be defined by the single datum with rainfall. When multiplied by the wind (indistinct average of the 6 data, 5 of which are non-simultaneous with rainfall), this minor precipitation weights the interval aDRI value, thus minimising the relevance of its co-occurrence error in the global aDRI analysis.

Thus, although the averaging error (e_2) is a secondary source of error for calculating the WDR exposure (i.e., aDRI value), it is clearly more influential than the co-occurrence error for the calculation of the DRWP exposure (Figs 5 and 6). Likewise, although co-occurrence errors (e_1) exhibit a similar influence on both exposure indices, this is slightly lower for the calculation of WDR exposure. For all of the above, the datasets used to characterise the DRWP exposure require a better time resolution than those employed for aDRI calculation if both characterisations are intended to have similar levels of uncertainty.

Fig. 5. Evolution of mean calculation errors in aDRI values for the usual time resolutions used for climate datasets (logarithmic scale).

Fig. 6. Evolution of mean calculation errors in DRWP values for the usual time resolutions used for climate datasets (logarithmic scale).

In summary, it can be said that the error committed (and also its dispersion or standard deviation) grows rapidly as the time resolution gets worse, stabilising for the monthly - annual resolution. Based on the 10-

min results, only the hourly datasets provide estimates of DRWP exposure with errors less than 11%. In the case of aDRI indices, only the hourly and daily datasets maintain an average error below this threshold. The distinct dataset time resolution required to calculate both exposures with a similar level of accuracy is thus shown. Those climate datasets with lower time resolution (i.e., monthly and annual datasets), although they significantly reduce the calculation effort and can provide a reasonable exposure ranking among diverse locations, should be used with caution owing to their high uncertainty.

The above suggests the need to perform a critical re-analysis of the WDR and DRWP characterisation studies performed so far using climate datasets with low time resolution. Given the representativeness of the study conditions (long series of records with less than 1.5% of missing data and locations with different conditions), the obtained error ranges can serve as guidelines for this re-analysis, assessing the uncertainty associated with the time resolution of the climatic datasets used in locations subject to different environmental conditions and exposure.

4.1 Fitting relationships.

In any case, climate datasets with exhaustive and simultaneous precipitation and wind speed records are often unavailable in many regions (the number of suitable weather stations is often insufficient, or the records cover a non- representative number of years). Therefore, several studies have identified simple linear regressions that allow extrapolating scalar values of WDR exposure associated with datasets of different time resolutions. In this manner, the possibility of improving the accuracy of the results obtained from deficient data series (e.g., from aaDRI or maDRI values, up to its corresponding daDRI estimation) exists.

In general, there is a great coincidence between the aaDRI-maDRI adjustments identified in different geographic areas, such as Nigeria, India, Brazil, Greece, Chile and Spain, with coefficients of determination higher than 0.95 (Akingbade 2004; Chand and Bhargava 2002; Domínguez et al. 2016;

Giarma and Aravantinos 2014; Pérez, Domínguez, Cano et al. 2013; Pérez, Domínguez, Rodríguez et al. 2012). However, Figs. 5 and 6 show that the improvement provided by these adjustments is not significant because the monthly indices maintain very high uncertainties, similar to the annual ones.

This coincidence between different regions is also maintained in the maDRI-daDRI and aaDRI-daDRI relationships: Fig. 7 compiles the linear regressions obtained from the results of the above mentioned studies that also analyse daily climate datasets. As observed, the adjustments associated with the 6 sites of Galicia are similar to those of the whole of Spain, in addition to those of other areas in middle latitudes, such as Greece and much of Chile. Brazil, located in a tropical zone and influenced by monsoon-type precipitations, presents a more divergent adjustment. This suggests that these adjustment relationships are related to the pluviometric and eolian patterns of each region, being similar in areas with similar climatic conditions (generically, mid-latitudes with seasonal rainfall).

Fig. 7. (a) Best-fit linear relationship between daDRI and maDRI; (b) best fit-linear relationship between daDRI and aaDRI, and its comparison with different countries.

For all of the above, it is presumed that the good correlations between the indices aaDRI-maDRI-daDRI also extend to scalar exposure indices obtained by datasets with a higher time resolution. Thus, Fig. 8 shows the simple linear regression between the 10-min indices of WDR exposure and those corresponding to other time resolutions for the 6 stations analysed. In all cases, the strong correlation exists, with coefficients of determination close to the unit (especially for haDRI-10'aDRI and daDRI-10'aDRI adjustments).

These relationships could be used in areas with a similar climate as a first approximation to estimate accurate scalar indices of WDR exposure via low-time-resolution datasets. However, because no similar studies have been developed in other geographical areas, their validity and reliability should still be

verified. It is up to subsequent studies to take on the challenge of analysing raw measurement data in other regions, verifying and refining, if appropriate, the proposed extrapolations.

Fig. 8. Best-fit linear relationship between 10'aDRI and aDRI indices of other time resolutions.

In turn, Fig. 9 presents the simple linear regression between the 10'DRWP index and the DRWP values associated with other dataset time resolutions, for the 6 stations analysed. Given the absence of specific studies on the DRWP exposure variable, in this case, it is not possible to compare the similarity between adjustments obtained in different geographic regions~~,~~ (not even between DRWP values based on datasets with low time resolution).

However, it is observed in Fig. 9 that the coefficients of determination identified for these weather stations are similar to those of the aDRI indices, surpassing 0.97 for the 10'DRWP-hDRWP and 10'DRWP-dDRWP adjustments. As expected, this R^2 coefficient increases in both exposure parameters by improving the time resolution of the dataset considered.

On the other hand, several previous studies have found strong correlations between the wind pressure of the location and the value of DRWP in places as diverse as Brazil, Chile and Spain itself (Domínguez et al. 2016; Pérez Domínguez, Cano et al. 2013; Pérez et al. 2014), reflecting the linkage of the DRWP value to the wind conditions of each site. Again, additional studies in other geographical areas will be necessary to verify that the proposed DRWP extrapolations can be used in regions with similar climatic conditions to those of this study.

Fig. 9. Best-fit linear relationship between 10'DRWP and DRWP indices of other time resolutions.

4. Conclusions

This manuscript analyses the effect of the time resolution of climate records on the accuracy of the semi-empirical scalar indices that characterise WDR and DRWP exposures. For this purpose, long series of 10-min, daily, monthly and annual records gathered at sites subject to different exposures and conditions have been used. Taking exhaustive 10-min records as a reference, this error analysis provides a broad perspective on the nature and magnitude of the uncertainties associated with each possible time resolution of the dataset.

The results indicate that the main source of error for the calculation of aDRI indices corresponds to the use of wind speed records that are not strictly simultaneous to precipitation events (co-occurrence error). However, the error due to the averaging of the meteorological variables in longer intervals is more significant for the DRWP calculation.

In general, the error is reduced by using climate records with a better time resolution. However, DRWP indices present greater sensitivity to the time resolution of the dataset, requiring higher time resolution to reduce their uncertainty range. Thus, the hourly and daily datasets may be considered sufficiently accurate to characterise the scalar WDR and DRWP exposures, respectively (with errors less than 11%). On the contrary, the monthly and annual climate records (in addition to the daily records for the calculation of the DRWP exposure) should be used with caution, owing to their high uncertainty. The results provided can be used as a guide to reinterpret scalar exposures already obtained through low-resolution datasets, in addition to estimate the accuracy of future results in which the available climate data do not reach the required quality. All this can be used to provide more reliable exposure data, thus improving the facade designs to reduce the risk of atmospheric water penetration.

In any case, fitting relationships capable of extrapolating accurate values of aDRI and DRWP (similar to those based on 10-min records), from low-resolution datasets have also been presented. The representativeness of the study conditions and their comparison with results obtained in other regions and

climates suggest that these relationships can be useful in other places with similar climatic conditions. Nevertheless, it is still necessary to validate and refine these extrapolations, which opens a new and interesting line of work for the study of raw meteorological data in different regions of the world.

References

Akingbade FOA (2004) Estimation of driving rain index for Nigeria. Archit Sci Rev 47(2):103-106. doi: 10.1080/00038628.2004.9697032.

American Architectural Manufacturers Association (2005) AAMA 501.1. Standard test method for water penetration of exterior windows, curtain walls and doors using dynamic pressure. AAMA, Schaumburg.

American Society for Testing and Materials (2009) ASTM E311-00. Standard test method for water penetration of exterior windows, skylights, doors, and curtain walls by uniform static air pressure difference. ASTM, West Conshohocken.

American Society of Heating and Air-Conditioning Engineers (2016) ANSI/ASHRAE Standard 160. Criteria for moisture-control design analysis in buildings. ASHRAE, Atlanta.

Blocken B, Carmeliet, J (2004) A review of wind-driven rain research in building science. J Wind Eng Ind Aerodyn 92(13):1079-1130. doi: 10.1016/j.jweia.2004.06.003.

Blocken B, Carmeliet J (2007) On the errors associated with the use of hourly data in wind-driven rain calculations on building facades. Atmos Environ 41:2335-2343. doi: 10.1016/j.atmosenv.2006.11.014.

Blocken B, Carmeliet J (2008) Guidelines for the required time resolution of meteorological input data for wind-driven rain calculations on buildings. J Wind Eng Ind Aerodyn 96:621-639. doi: 10.1016/j.jweia.2008.02.008.

Blocken B, Derome J, Carmeliet J (2013) Rainwater runoff from building facades: A review. Build Environ 60:339-361. doi: 10.1016/j.buildenv.2012.10.008.

Chand I, Bhargava PK (2002) Estimation of driving rain index for India. Build Environ 37(5):549-554. doi: 10.1016/S0360-1323(01)00057-9.

Cornick SM, Dalgliesh A, Said N, Djebbar R, Tariku F, Kumaran MK (2002) Report from Task 4 of MEWS Project: Task 4 – Environmental conditions final report (Research Report No. 113). National Research Council Canada, Ottawa.

Cornick SM, Lacasse MA (2005) A review of climate loads relevant to assessing the watertightness performance of walls, windows, and wall-window interfaces. J ASTM Int 2(10):1-16. doi: 10.1520/JAI12505.

D'ayala D, Aktas YD (2016) Moisture dynamics in the masonry fabric of historic buildings subjected to wind-driven rain and flooding. Build Environ 104(1):208-220. doi: 10.1016/j.buildenv.2016.05.015.

Dell'Isola M, D'Ambrosio FR, Giovinco GE, Ianniello E (2013) Experimental analysis of thermal conductivity for building materials depending on moisture content. Int J Thermophys 33:1674-1685. doi: 10.1007/s10765-012-1215-z.

De Souza JS, Bauer E, Nascimento MLM, Capuzzo VMS, Zanoni VAG (2016) Study of damage distribution and intensity in regions of the facade. J Build Rehabil 1:3. doi: doi:10.1007/s41024-016-0003-8.

Domínguez J, Pérez JM, Alonso M, Cano E, del Coz JJ (2016) Assessment of water penetration risk in building facades throughout Brazil. Build Res Inf, In press. doi: 10.1080/09613218.2016.1183441.

Erkal A, D'Ayala D, Sequeira L (2012) Assessment of wind-driven rain impact, related surface erosion and surface strength reduction of historic building materials. Build Environ 57:336-348. doi: 10.1016/j.buildenv.2012.05.004.

European Committee for Standardization (2001) EN 12865. Hygrothermal performance of building components and building elements. Determination of the resistance of external wall systems to driving rain under pulsating air pressure. CEN, Brussels.

European Committee for Standardization (2009) EN ISO 15927-3. Hygrothermal performance of buildings.Calculation and presentation of climatic data. Part 3: calculation of a driving rain index forvertical surfaces from hourly wind and rain data. CEN, Brussels.

Ge H (2015) Influence of time resolution and averaging techniques of meteorological data on the estimation of wind-driven rain load on building facades for Canadian climates. J Wind Eng Ind Aerodyn 143:50-61. doi: 10.1016/j.jweia.2015.04.019.

Giarma C, Aravantinos D (2011) Estimation of building components' exposure to moisture in Greece based on wind rainfall and other climatic data. J Wind Eng Ind Aerodyn 99:91-102. doi: 10.1016/j.jweia.2010.12.001.

Giarma C, Aravantinos D (2014) On building components' exposure to driving rain in Greece. J Wind Eng Ind Aerodyn 125:133-145. doi: 10.1016/j.jweia.2013.11.014.

Gutiérrez R, Gutiérrez-Sánchez R, Nafidi A (2008) Trend analysis using nonhomogeneous stochastic diffusion processes. Emission of CO_2; Kyoto protocol in Spain. Stoch Environ Res Risk Assess 22(1):57-66. doi: 10.1007/s00477-006-0097-7.

Hall C, Hoff WD (2012) Water transport in brick, stone and concrete. 2nd ed. Spon Press, New York.

Hangan HJV (1999) Wind-driven rain simulations. J Vis 1(4):337-343. doi:10.1007/BF03181423.

Hoppestad S (1955) Slagregninorge (Driving rain in Norway, in Norwegian). Norwegian Building Research Institute Report no. 13. NBI, Oslo.

Jones DMA, Sims AL (1978) Climatology of instantaneous rainfall rates. J Appl Meteorol 17:1135-1150. doi: 10.1175/1520-0450(1978)017<1135:COIRR>2.0.CO;2.

Kočí V, Vejmelková E, Čáchová M, Koňáková D, Keppert M, Maděra J, Černý R (2017) Effect of moisture content on thermal properties of porous building materials. Int J Thermophys 38:28. doi:10.1007/s10765-016-2164-8.

Kottek M, Grieser J, Beck C, Rudolf B, Rubel F (2006) World map of the Köppen-Geiger climate classification updated. Meteorol Z 15:259-63. doi: 10.1127/0941-2948/2006/0130.

Lacasse MA, O'Connor T, Nunes SC, Beaulieu P (2003) Report from Task 6 of MEWS Project: Experimental assessment of water penetration and entry into wood-frame wall specimens – Final Report (Institute for Research in Construction - Internal Report 113). National Research Council Canada, Ottawa.

Lacy RE, Shellard HC (1962) An index of driving rain. Meteorol Mag 91(1080):177-184.

Mornet A, Opitz T, Luzi M. Loisel S, Bailleul B (2016) Wind storm risk management: sensitivity of return period calculations and spread on the territory. Stoch Environ Res Risk Assess (in press). doi:10.1007/s00477-016-1367-7

Nascimento MLM, Bauer E, de Souza JS, Zanoni VAG (2016). Wind-driven rain incidence parameters obtained by hygrothermal simulation. J Build Rehabil 1:5. doi: 10.1007/s41024-016-0006-5.

Pérez JM, Domínguez J, Cano E, del Coz JJ, Alonso M (2013) Global analysis of building façade exposure to water penetration in Chile. Build Environ 70:284-297. doi: 10.1016/j.buildenv.2013.09.001.

Pérez JM, Domínguez J, Cano E, del Coz JJ, Martín A (2014) Procedure for a detailed territorial assessment of wind-driven rain and driving-rain wind pressure and its implementation to three Spanish regions. J Wind Eng Ind Aerodyn 128:76-89. doi: 10.1016/j.jweia.2014.02.008.

Pérez JM, Domínguez J, Rodríguez B, del Coz JJ, Cano E (2012) Estimation of the exposure of buildings to driving rain in Spain from daily wind and rain data. Build Environ 57:259-270. doi: 10.1016/j.buildenv.2012.05.010.

Pérez JM, Domínguez J, Rodríguez B, del Coz JJ, Cano E (2013) Combined use of wind-driven rain and wind pressure to define water penetration risk into building façades: The Spanish case. Build Environ 64:46-56. doi: 10.1016/j.buildenv.2013.03.004.

Sahal AN, Lacasse MA (2004). Experimental assessment of water penetration and entry into siding-clad wall specimen (Internal Report No. 862). Institute forResearch in Construction, National Research Council Canada, Ottawa.

Skerlj PF (1999) A Critical assessment of the driving rain wind pressures used in CSA Standard CAN/CSA-A44-M90. M.A.Sc. Thesis, Faculty of Engineering Science, University of Western Ontario, London.

Straube JF, Burnett EFP (2000) Simplified prediction of driving rain deposition. In: Proceedings of International Building Physics Conference, Eindhoven, pp 375-382.

Sumner G (1988) Precipitation: Process and analysis. John Wiley & Sons, New York.

Tang W, Davidson CI, Finger S, Vance K (2004) Erosion of limestone building surfaces caused by wind-driven rain. 1. Field measurements. Atmos Environ 38(33):5589-5599. doi: 10.1016/j.atmosenv.2004.06.030.

Van de Vyver H (2015). On the estimation of continuous 24-h precipitation maxima. Stoch Environ Res Risk Assess 29:653-663. doi:10.1007/s00477-014-0912-5

Van der Hoven I (1957) Power sprectrum of horizontal wind speed in the frequency range from 0.0007-900 cycles per hour. J Meteorol 14:160-164. doi: 10.1175/1520-0469(1957)014<0160:PSOHWS>2.0.CO;2.

Welsh RE, Skinner WR, Morris RJ (1989) A climatology of driving rain pressure for Canada (Climate and Atmospheric Research Directorate Draft Report). Environment Canada, Atmospheric Environment Service, Gatineau.

World Health Organization (2011) Environmental burden of disease associated with inadequate housing. Methods for quantifying health impacts of selected housing risks in the WHO European region. WHO, Copenhagen.

World Meteorological Organization (2008) Guide to Meteorological Instruments and Methods of Observation. WMO-No 8. WMO, Geneva.

Xunta of Galicia (2017) Department of Environment, Territory and Infrastructures. Galicia, Spain. http://www.meteogalicia.gal/. Accessed 19 May 2017.

Figure captions

Fig. 1. Characteristics and location of the 6 analysed weather stations.

Fig. 2. Location of the 6 weather stations selected for the conducted study. *Darker colours represent higher elevations.*

Fig. 3. Magnitude and nature of the aDRI error associated with each time resolution and its fluctuation for the different analysed locations.

Fig. 4. Magnitude and nature of the DRWP error associated with each time resolution and its fluctuation for the different analysed locations.

Fig. 5. Evolution of mean calculation errors in aDRI values for the usual time resolutions used for climate datasets (logarithmic scale).

Fig. 6. Evolution of mean calculation errors in DRWP values for the usual time resolutions used for climate datasets (logarithmic scale).

Fig. 7. (a) Best-fit linear relationship between daDRI and maDRI; (b) best fit-linear relationship between daDRI and aaDRI, and its comparison with different countries.

Fig. 8. Best-fit linear relationship between 10'aDRI and aDRI indices of other recording intervals.

Fig. 9. Best-fit linear relationship between 10'DRWP and DRWP indices of other recording intervals.

CIS Ferrol
(Ferrol city municipality)
Coastal zone / drowned river valley
Altitude: 37 m
Rain gauge: R.M.Young 52202/03
Average rainfall: 1,257 mm/year
Anemometer: Ornytion 107H4M
Mean wind speed: 3.14 m/s
Missing data: 0.98%

Pedro Murias
(Ribadeo municipality)
Coastal zone / drowned river valley
Altitude: 51 m
Rain gauge: R.M.Young 52202/03
Average rainfall: 986 mm/year
Anemometer: Ornytion 107U
Mean wind speed: 2.94 m/s
Missing data: 0.65%

Corrubedo
(Ribeira municipality)
Coastal zone
Altitude: 30 m
Rain gauge: R.M.Young 52202/03
Average rainfall: 1,056 mm/year
Anemometer: R.M.Young 05106
MA Mean wind speed: 4.09 m/s
Missing data: 1.22%

Campus Lugo
(Lugo city municipality)
Inland / urban environment
Altitude: 400 m
Rain gauge: Campbell ARG100
Average rainfall: 948 mm/year
Anemometer: Ornytion 107U
Mean wind speed: 1.79 m/s
Missing data: 0.57%

Queimadelos
(Mondariz municipality)
Forest zone
Altitude: 371 m
Rain gauge: Campbell ARG100
Average rainfall: 1,785 mm/year
Anemometer: Ornytion 107H/4
Mean wind speed: 1.37 m/s
Missing data: 0.46%

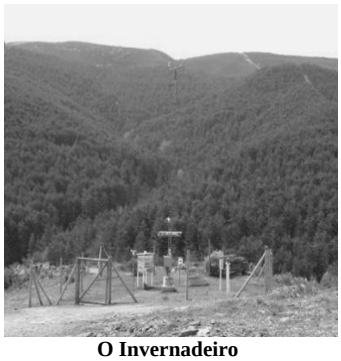

O Invernadeiro
(Vilariño de Conso municipality)
Inland / mountain zone
Altitude: 1026 m
Rain gauge: Thies 5.4032.35.007
Average rainfall: 1,651 mm/year
Anemometer: Ornytion 107U
Mean wind speed: 2.30 m/s
Missing data: 1.50%

Fig. 1. Characteristics and location of the 6 analysed weather stations.

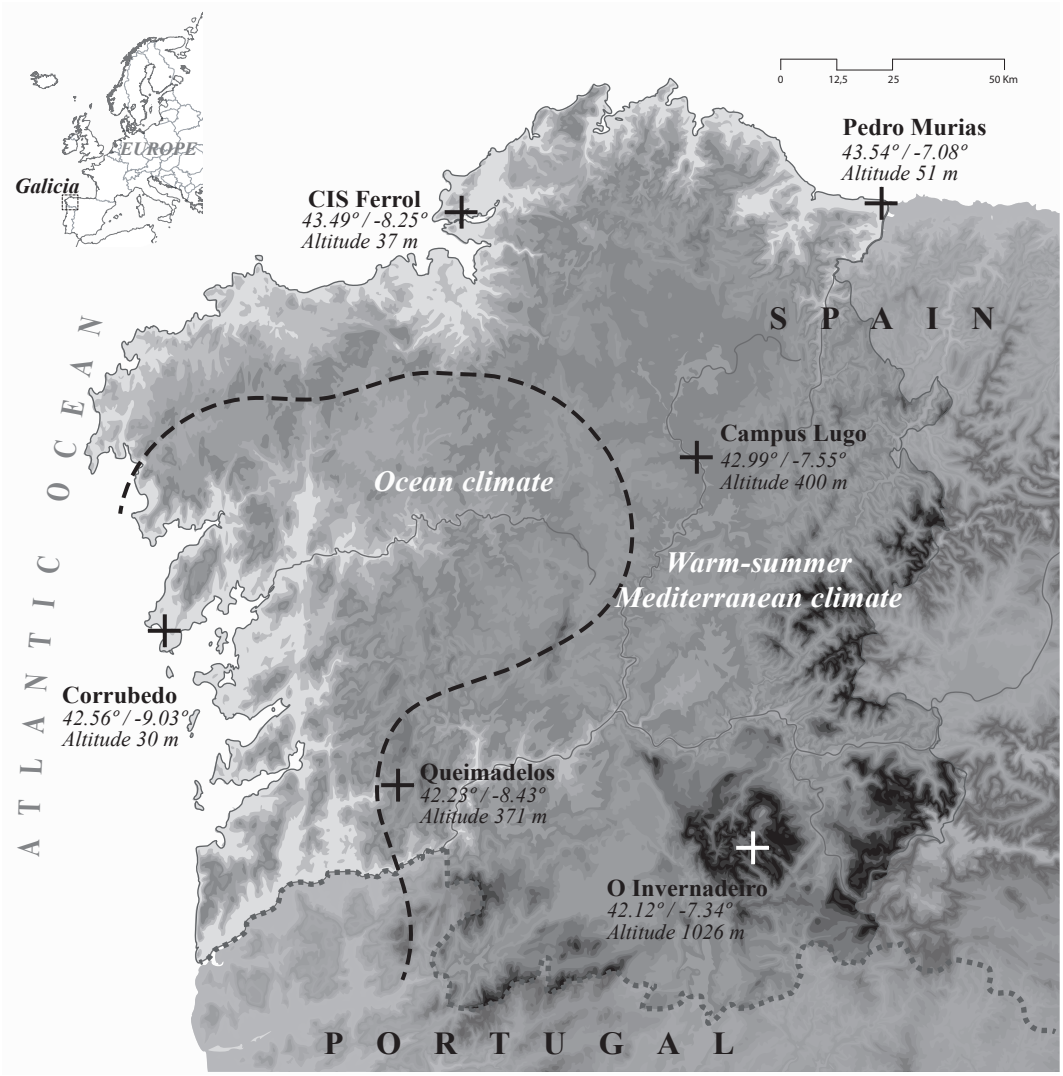

Fig. 2. Location of the 6 weather stations selected for the conducted study. *Darker colours represent higher elevations.*

Figure 3

Click here to download line figure Figure 3_R1.eps

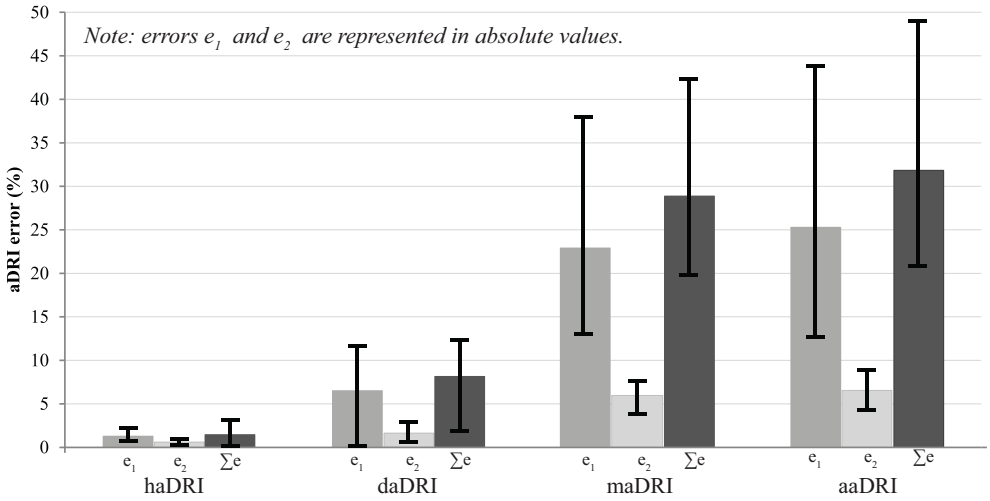

Fig. 3. Magnitude and nature of the aDRI error associated with each time resolution and its fluctuation for the different analysed locations.

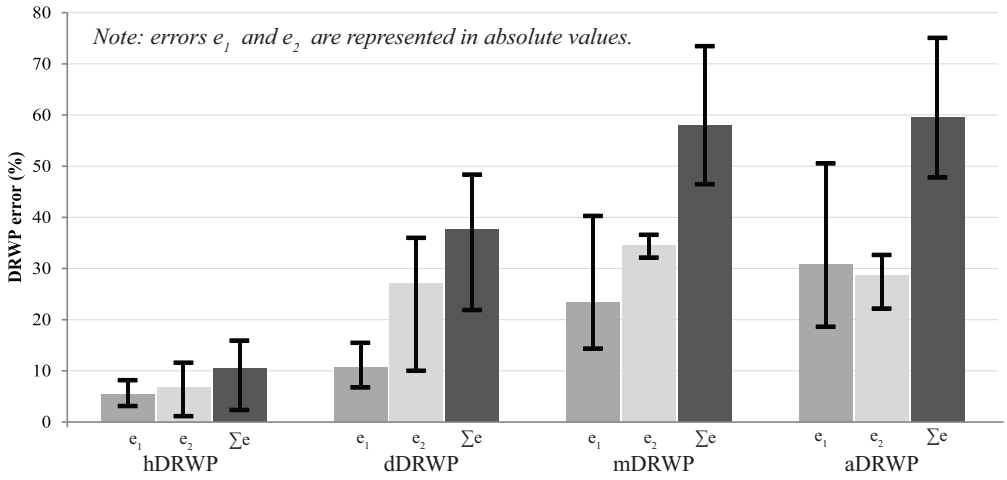

Fig. 4. Magnitude and nature of the DRWP error associated with each time resolution and its fluctuation for the different analysed locations.

Figure 5 Click here to download line figure Figure 5_R1.eps

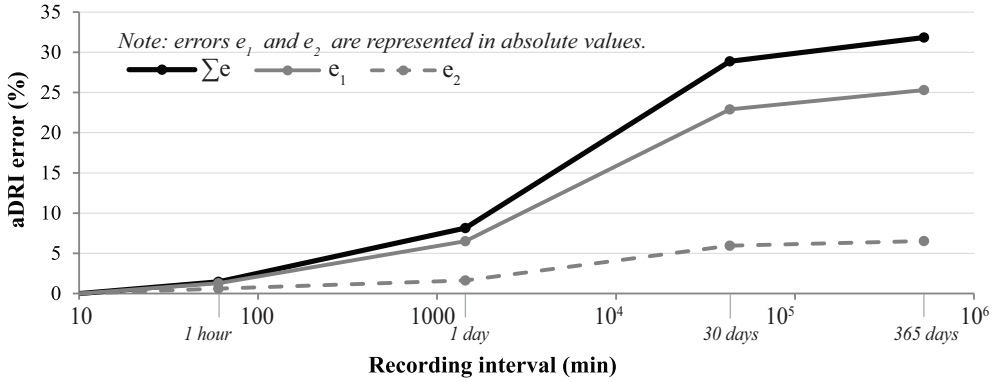

(%)	Hourly dataset	Daily dataset	Monthly dataset	Annual dataset
Total mean error	1.46	8.15	28.87	31.83
Standard deviation	*1.2*	*4.0*	*8.8*	*10.6*
Mean error e_1	1.28	6.51	22.91	25.30
Standard deviation	*0.6*	*4.2*	*9.3*	*11.3*
Mean error e_2	0.61	1.64	5.96	6.54
Standard deviation	*0.3*	*0.8*	*1.5*	*1.5*

Fig. 5. Evolution of mean calculation errors in aDRI values for the usual time resolutions used for climate datasets (logarithmic scale).

Figure 6 Click here to download line figure Figure 6_R1.eps

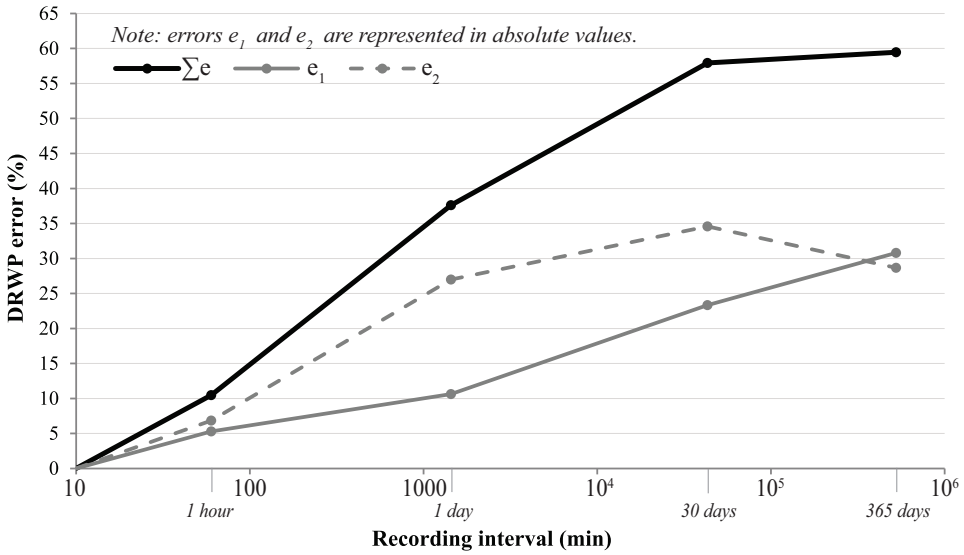

(%)	Hourly dataset	Daily dataset	Monthly dataset	Annual dataset
Total mean error	10.48	37.62	57.92	59.47
Standard deviation	*4.9*	*10.7*	*10.1*	*9.9*
Mean error e_1	5.29	10.62	23.33	30.81
Standard deviation	*1.9*	*3.4*	*10.4*	*13.4*
Mean error e_2	6.85	27.00	34.59	28.66
Standard deviation	*3.8*	*10.9*	*1.7*	*4.4*

Fig. 6. Evolution of mean calculation errors in DRWP values for the usual time resolutions used for climate datasets (logarithmic scale).

Figure 7 Click here to download line figure Figure 7.eps

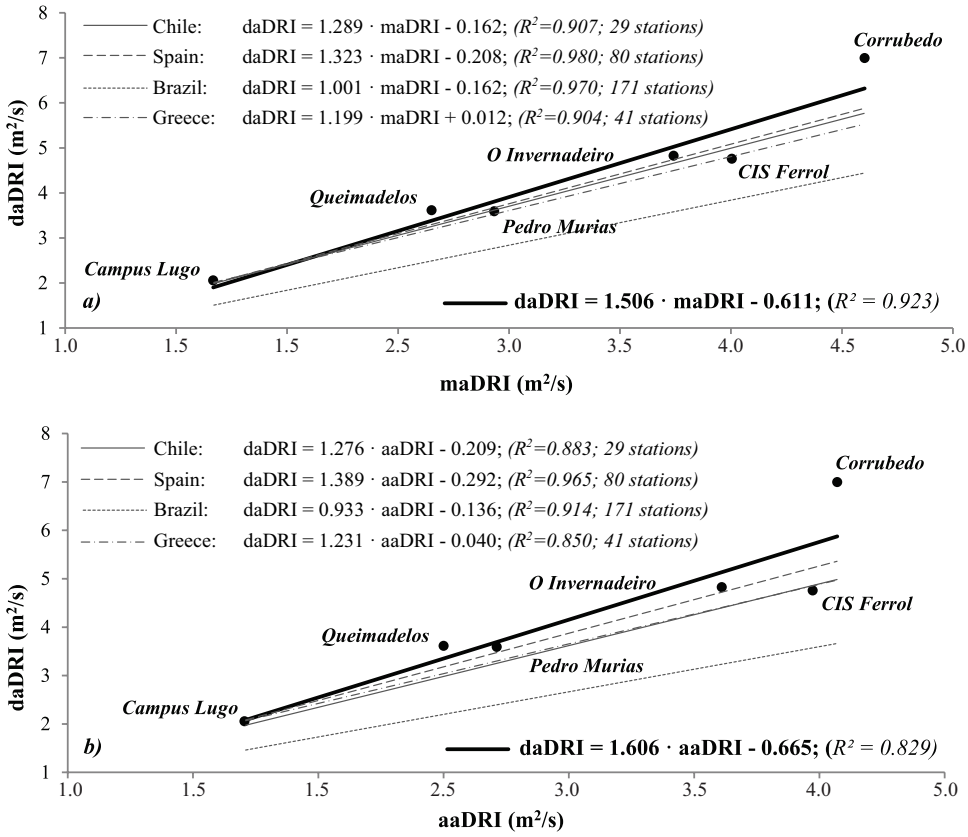

Fig. 7. a) Best-fit linear relationship between daDRI and maDRI; b) best fit-linear relationship between daDRI and aaDRI, and its comparison with different countries.

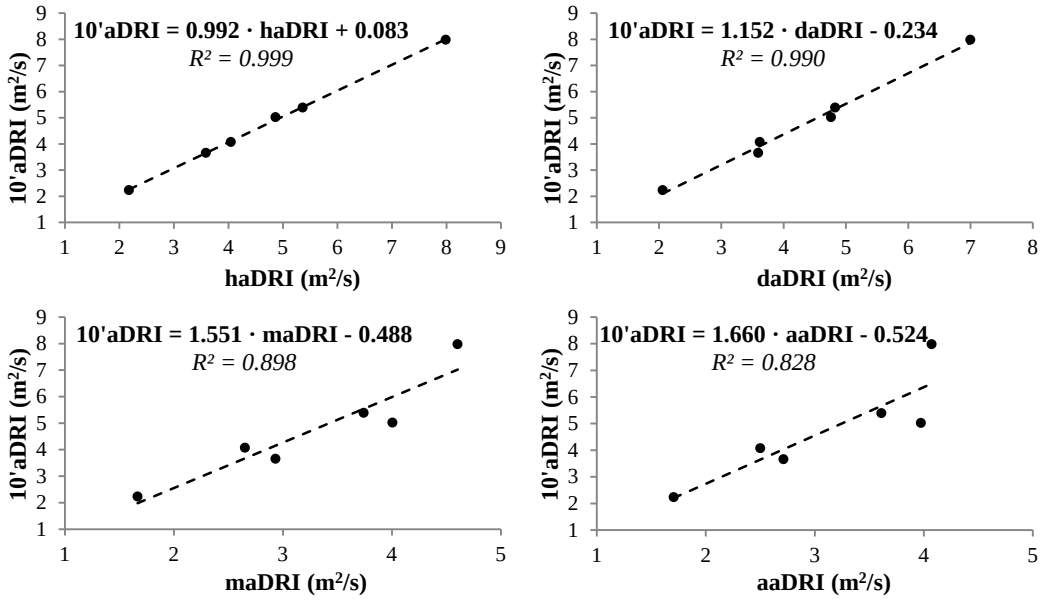

Fig. 8. Best-fit linear relationship between 10'aDRI and aDRI indices of other time resolutions.

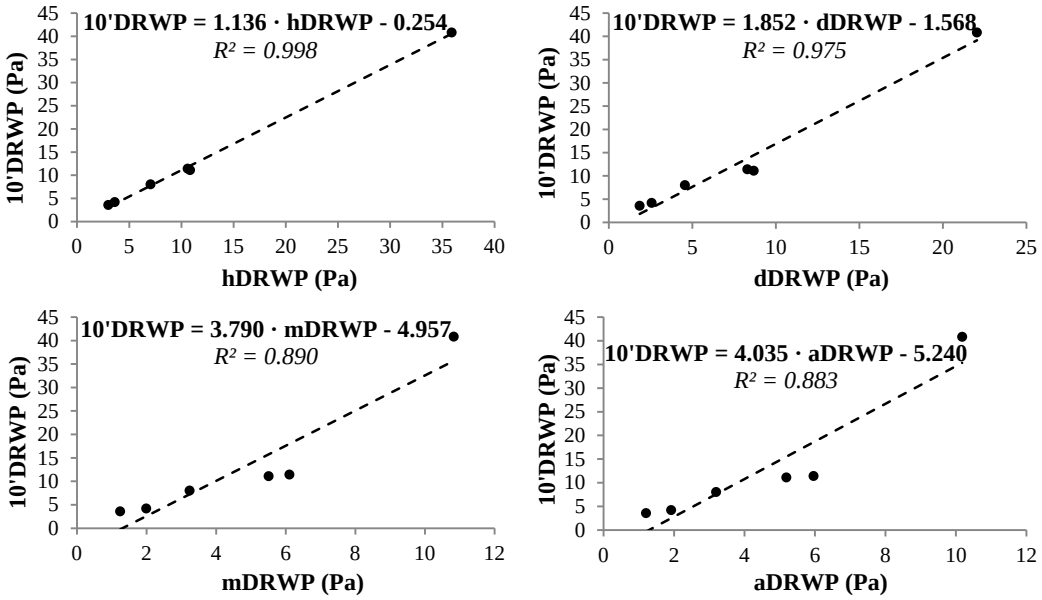

Fig. 9. Best-fit linear relationship between 10'DRWP and DRWP indices of other time resolutions.

List of tables

Table 1.
Exposure results to wind-driven rain and simultaneous wind pressure for climate datasets of different time resolution.

aDRI (m^2/s)	CIS Ferrol	Pedro Murias	Corrubedo	Campus Lugo	Quimadelos	O Invernadeiro
10'aDRI	**5.02**	**3.66**	**7.98**	**2.23**	**4.07**	**5.39**
haDRI	4.86	3.59	7.99	2.18	4.05	5.36
daDRI	4.76	3.59	7.00	2.06	3.62	4.83
maDRI	4.00	2.93	4.60	1.67	2.65	3.74
aaDRI	3.97	2.71	4.07	1.71	2.50	3.61

DRWP (Pa)	CIS Ferrol	Pedro Murias	Corrubedo	Campus Lugo	Quimadelos	O Invernadeiro
10'DRWP	**11.41**	**11.10**	**40.82**	**4.20**	**3.57**	**8.02**
hDRWP	10.61	10.84	35.90	3.63	3.00	7.06
dDRWP	8.29	8.67	22.04	2.56	1.84	4.56
mDRWP	6.11	5.51	10.83	1.99	1.24	3.24
aDRWP	5.96	5.19	10.18	1.92	1.20	3.19

Table 2.
Exposure results without co-occurrence error for climate datasets with different time resolutions.

$aDRI_{e2}$ (m^2/s)	CIS Ferrol	Pedro Murias	Corrubedo	Campus Lugo	Quimadelos	O Invernadeiro
10'aDRI	**5.02**	**3.66**	**7.98**	**2.23**	**4.07**	**5.39**
haDRI$_{e2}$	4.97	3.63	8.05	2.22	4.08	5.40
daDRI$_{e2}$	4.97	3.60	7.93	2.17	3.99	5.30
maDRI$_{e2}$	4.66	3.52	7.63	2.06	3.80	5.06
aaDRI$_{e2}$	4.61	3.50	7.56	2.06	3.80	5.01

$DRWP_{e2}$ (Pa)	CIS Ferrol	Pedro Murias	Corrubedo	Campus Lugo	Quimadelos	O Invernadeiro
10'DRWP	**11.41**	**11.10**	**40.82**	**4.20**	**3.57**	**8.02**
hDRWP$_{e2}$	11.54	11.53	37.18	3.89	3.15	7.35
dDRWP$_{e2}$	9.49	9.99	28.36	2.85	2.28	5.10
mDRWP$_{e2}$	7.74	7.20	27.27	2.67	2.35	5.09
aDRWP$_{e2}$	8.08	7.50	30.81	2.83	2.78	5.53

Table 3.
Percentage errors derived from the non-co-occurrence of wind and rain (e_1) and from the averaged data (e_2) for climate datasets of different time resolution (regarding 10-min values).

	haDRI			daDRI			maDRI			aaDRI		
	e_1	e_2	e_1+e_2	e_1	e_2	e_1+e_2	e_1	e_2	e_1+e_2	e_1	e_2	e_1+e_2
CIS Ferrol	-2.2	-0.9	-3.1	-4.3	-0.9	-5.2	-13.1	-7.2	-20.9	-12.7	-8.2	-20.9
Pedro Murias	-1.2	-0.7	-1.9	-0.2	-1.6	-1.8	-16.0	-3.9	-19.8	-21.6	-4.3	-25.9
Corrubedo	-0.7	+0.8	+0.1	-11.7	-0.6	-12.3	-38.0	-4.4	-42.3	-43.8	-5.2	-49.0
Campus Lugo	-1.9	-0.7	-2.5	-5.0	-2.9	-7.9	-17.8	-7.6	-25.4	-16.1	-7.6	-23.6
Queimadelos	-0.9	+0.3	-0.7	-9.2	-2.1	-11.2	-28.3	-6.6	-34.9	-31.8	-6.8	-38.6
O Invernadeiro	-0.7	+0.3	-0.4	-8.8	-1.7	-10.4	-24.4	-6.1	-30.6	-25.9	-7.1	-33.0

	hDRWP			dDRWP			mDRWP			aDRWP		
	e_1	e_2	e_1+e_2	e_1	e_2	e_1+e_2	e_1	e_2	e_1+e_2	e_1	e_2	e_1+e_2
CIS Ferrol	-8.2	+1.1	-7.0	-10.5	-16.9	-27.4	-14.3	-32.1	-46.5	-18.6	-29.2	-47.8
Pedro Murias	-6.2	+3.8	-2.3	-11.8	-10.0	-21.9	-15.2	-35.1	-50.4	-20.8	-32.4	-53.3
Corrubedo	-3.1	-8.9	-12.0	-15.5	-30.5	-46.0	-40.3	-33.2	-73.5	-50.6	-24.5	-75.1
Campus Lugo	-6.4	-7.2	-13.5	-6.7	-32.2	-38.9	-16.2	-36.3	-52.5	-21.6	-32.7	-54.3
Queimadelos	-4.3	-11.6	-15.9	-12.4	-36.0	-48.4	-30.9	-34.2	-65.1	-44.1	-22.2	-66.2
O Invernadeiro	-3.6	-8.4	-12.0	-6.8	-36.4	-43.2	-23.0	-36.6	-59.6	-29.2	-31.0	-60.2